THE JOURNAL OF PHYSICAL CHEMISTRY C

Article

pubs.acs.org/JPCC

Reversible Hydrogenation Studies of $NaBH_4$ Milled with Ni-Containing Additives

Terry D. Humphries,* Georgios N. Kalantzopoulos, Isabel Llamas-Jansa, Jørn Eirik Olsen, and Bjørn C. Hauback

Institute for Energy Technology, Physics Department, P.O. Box 40, NO-2027, Kjeller, Norway

Supporting Information

ABSTRACT: $NaBH_4$ has long been identified as a viable hydrogen-storage material due to a theoretical gravimetric H_2 capacity of 10.6 wt %. Because of the high enthalpy of decomposition of 108 ± 3 kJ mol^{-1}, thermal decomposition of the pristine material does not occur until at least 500 °C, and thus $NaBH_4$ has yet to be utilized in hydrogen-storage processes. In this study, $NaBH_4$ has been milled with a variety of Ni-containing additives to investigate the effects on the temperatures required for thermal desorption of H_2 by temperature-programmed desorption measurements and the products characterized by powder X-ray diffraction (PXD). Ni-containing additives have been determined to significantly enhance the thermal desorption of H_2 by at least 60 °C (Ni (65 wt %)) on Si/Al_2O_3. PCT cycling experiments have been conducted to ascertain their effects on the reversible hydrogenation of the milled $NaBH_4$. PXD analysis indicates that Ni reacts with B evolved during thermal decomposition to form Ni_xB_y species including Ni_3B, Ni_2B, and Ni_3B_4. A catalyst screening study of $NaBH_4$ with a variety of nanoparticles, chlorides, borides, and mesoporous materials has also been conducted, the most effective of which has been found to be Pd nanoparticles, which have a desorption temperature of 420 °C, a decrease of at least 85 °C.

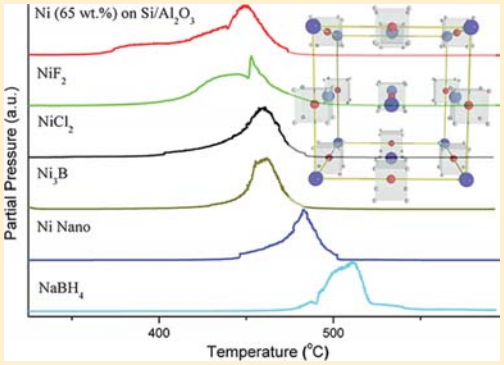

1. INTRODUCTION

The practical utilization of hydrogen as an energy carrier for on-board applications awaits the development of high-capacity hydrogen storage materials that can be recharged under moderate conditions. A viable on-board hydrogen carrier must have high gravimetric and volumetric hydrogen capacities, thermodynamic properties that are within rather stringent limits, and dehydrogenation and rehydrogenation kinetics that allow hydrogen cycling at relatively low temperatures and pressures.[1,2] One of the most important breakthroughs in the development of hydrogen storage materials in the past 20 years was provided by Bogdanović and Schwickardi, whose pioneering studies demonstrated that upon the addition of selected titanium compounds the dehydrogenation of $NaAlH_4$ is kinetically enhanced and rendered reversible under moderate conditions in the solid state.[3] Borohydrides have recently been in the forefront of many publications, mainly due to their large gravimetric and volumetric H_2 capacities, rich chemistry, and relative ease of synthesis.[4−7] The alkali metal borohydrides (Li, Na, and K) are commercially available and relatively inexpensive, enabling much research to be conducted into the fundamental science of the molecules and the preparation of many novel borohydrides.[8]

$NaBH_4$ theoretically contains 10.6 wt % H_2 with a volumetric density of 113 kg of H_2 m^{-3} but with an enthalpy and entropy of reaction of 108 ± 3 kJ mol^{-1} H_2 and 133 ± 3 J K^{-1} mol^{-1} H_2 released, respectively. This corresponds to a decomposition temperature of 534 ± 10 °C at 1 bar H_2.[9] The thermal decomposition of $NaBH_4$ is a one-step process with Na and B being the products and releasing only H_2 gas (eq 1). The effectiveness of Ti-containing additives toward the reversible hydrogenation of $NaAlH_4$[10] and $LiAlH_4$[11,12] has prompted the investigation of these additives toward the thermal decomposition of borohydride complexes including $LiBH_4$,[5,13] $Ca(BH_4)_2$, and $Mg(BH_4)_2$,[4] which has proven to have limited success under moderate conditions. Mao et al. recently published a study using Ti-containing additives. which decreases the temperatures required for decomposition.[14] TiF_3 was notably the most efficient additive, causing an onset of decomposition below 330 °C. The enhanced thermodynamics are attributed to the formation of TiB_2 and NaF during decomposition, which interact with $NaBH_4$ to catalyze the decomposition process. Mao et al. also note that the Ti additives provide a pathway toward reversibility. Mixtures of NaH and B were milled with Ti-containing additives and placed under 5.5 MPa of H_2 at 500 °C. TiF_3 was the most effective additive with absorption of 4.0 wt % H_2. $NaBH_4$ was observed by PXD and FT-IR, along with the formation of a $NaF_{1-x}H_x$ phase and TiH_2, which are assumed to aid the hydrogenation process.

Received: December 9, 2012
Revised: February 22, 2013

   dx.doi.org/10.1021/jp312105w | J. Phys. Chem. C XXXX, XXX, XXX−XXX

$$NaBH_4 \rightarrow Na + B + 2H_2 \quad (1)$$

Herein, the effects of Ni-containing additives on the thermal decomposition of $NaBH_4$ have been explored by PXD, DSC, TGA, and TPD and were found to be very effective compared with other borides, chlorides, nanoparticles, and mesoporous materials. A PCT cycling study (dehydrogenation and hydrogenation were conducted four times consecutively) was conducted to ascertain whether $NaBH_4$ mechano-milled with Ni additives were able to be reversibly hydrogenated and whether the activity of the additive increases over time.

2. EXPERIMENTAL SECTION

Samples of $NaBH_4$ (Sigma Aldrich 98.5%) were ball-milled with selected nanoparticles (2 mol %), mesoporous catalysts (10 wt %, except for $TiSiO_4$, which was milled with 2 mol %), transition-metal chlorides (2 mol %), or transition-metal borides (2 mol %). The selected nanoparticle dopants were Ni (20 nm), Ti (65 nm), Al (80 nm), Pd (25 nm), diamond (Aldrich, <10 nm), Cr (30 nm), Fe (25 nm), and Ag (30−50 nm). The mesoporous catalysts and transition-metal chlorides were purchased from Sigma Aldrich: $TiSiO_4$ (99.8%, nanoparticles), Rh (5 wt % on activated alumina), Pt (5 wt % on alumina), Ni (65 wt % on Silicon and alumina), $TaCl_5$ (99.999%), $ReCl_3$, and $NiCl_2$ (99.99%). The Ni_3B, Co_3B, and V_3B were synthesized in-house, whereas TaB, TiB, and NiB (99%) were purchased from Sigma Aldrich. For screening purposes, all samples were treated equally. Milling was conducted in a Fritsch Pulverisette 7 planetary micro mill employing tempered steel vials and balls in an Ar atmosphere. A ball-to-powder ratio of 40:1 was employed, with a milling time of 1 h at a speed of 280 rpm. The resultant powder was manipulated in MBraun Unilab glove boxes filled with purified argon (<1 ppm O_2, H_2O) to avoid contamination.

PXD patterns were collected in transmission mode using Cu−$K_{a1,a2}$ (λ = 1.5418 Å) radiation in a Bruker AXS D8 advance diffractometer equipped with a Göbbel mirror and a LynxEye 1D strip detector. The diffraction patterns were obtained using rotating boron glass capillaries filled and sealed under an Ar atmosphere. Small amounts of pure Si were added as internal standard (ABCR, APS 1−5 μm, 99.999%). Acquisition of data was restricted to 2θ = 5−80°, with $\Delta 2\theta$ = 0.02° and 2 s/step scanning rates.

TPD was performed under dynamic vacuum up to 600 °C using an in-house built setup. A 2 °C/min heating rate and ∼20 mg of sample were used for all measurements. The gas release was analyzed with a MKS MicroVision Plus RGA.

PCT cycling experiments were performed using an in-house-built setup. Approximately 300 mg of sample was loaded into the sample holder and placed under static vacuum. The temperature at which samples was desorbed was the maximum temperature of desorption measured by TPD measurements (Table 1). The temperature in which the sample was kept during hydrogenation was calculated by the onset of desorption measured during the TPD measurements. A hydrogenation pressure of 100 bar was generally used.

Combined DSC and TGA measurements were conducted using a Netzsch STA 449 F3 analyzer. Approximately 15 mg of sample was loaded into alumina crucibles. Samples were heated to 600 °C at a heating rate of 2°/min. The flow rate of the Ar purge gas was set to 15 mL/min.

Synthesis of Ni_3B was carried out similar to that described by Kapfenberger et al.[15] An aqueous 2 M solution of $NaBH_4$ was added dropwise to an ice-cooled 0.27 M aqueous solution of $NiCl_2$ over 45 min, during which effervescence and a black precipitate was observed. The precipitate was then collected by filtration and washed with water and then EtOH. The amorphous solid was allowed to dry in air overnight, giving a yield of 62%. The identity of the amorphous powder was confirmed by PXD after annealing a small quantity at 350 °C for 1.3 h. PXD analysis indicated the presence of Ni_3B as the major phase (ICDD PDF 00-001-1260) and some Ni, likely from slight decomposition. The amorphous powder was employed as the additive material. The DSC measurements also complemented those previously published.[15] The analogous Co_3B and V_3B were prepared in an identical manner, although crystalline samples for PXD measurements were not observed.

Table 1. Decomposition Temperatures of $NaBH_4$ Samples with Nanoparticles (2 mol %), Transition-Metal Chlorides (2 mol %), Transition-Metal Borides (2 mol %), and Mesoporous Powders (10 wt %) Measured by TPD Analysis[a]

dopant	TPD (peak max) °C
Pd (nano)	420
Ni (65 wt %) on Si/Al_2O_3	449
NiF_2	453
$TaCl_5$	460
$NiCl_2$	460
Ni_3B	462
$ReCl_3$	465
Rh (5 wt %) on Al_2O_3	476
V_3B	478
Co_3B	480
Ni (nano)	483
$TiSiO_4$	489
Ti (nano)	493
TiB_2	503
Al (nano)	508
diamond (nano)	511
Ag (nano)	511
Cr (nano)	519
Pt (5 wt %) on act. Al_2O_3	523
Fe (nano)	527
pure $NaBH_4$	510

[a]Samples are ranked from lowest decomposition temperature to highest. Graphical illustration of data can be found in the Supporting Information (SI).

3. RESULTS AND DISCUSSION

3.1. PXD Analysis of Milled Materials. PXD analysis was conducted on all of the milled samples with Ni-containing additives with the addition of a Si standard (Figure 1). Analysis of the diffraction patterns of the $NaBH_4$ samples indicates that no reaction has taken place between the starting materials as the peak positions for $NaBH_4$ have not altered compared with those for pure $NaBH_4$. Identification of Ni metal in the diffraction patterns of mixtures containing Ni nanoparticles and also Ni (65 wt %) in Si/Al_2O_3 confirmed that no reaction had taken place. The Ni_3B additives are not expected to be visualized in the PXD patterns due to the amorphous nature of these compounds.[15]

3.2. Thermal Decomposition Studies. TPD-RGA analysis was conducted to determine the decomposition

dx.doi.org/10.1021/jp312105w | J. Phys. Chem. C XXXX, XXX, XXX−XXX

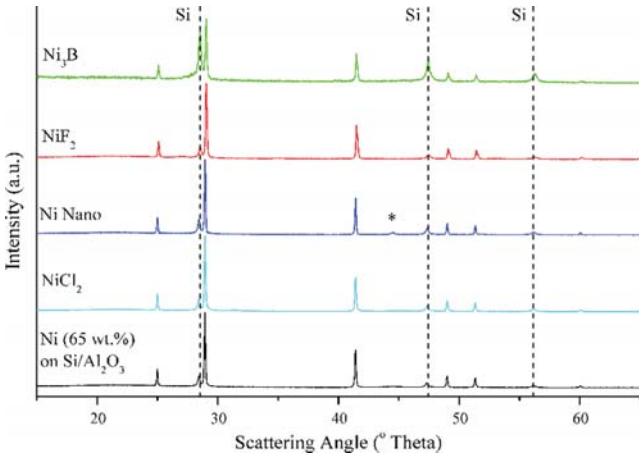

Figure 1. PXD analysis of $NaBH_4$ milled with Ni_3B, NiF_2, Ni nanoparticles, $NiCl_2$, and Ni (65 wt %) on Si/Al_2O_3. Samples were mixed with Si standard. * indicates the peak for Ni metal. λ = 1.5418 Å.

temperatures of the milled $NaBH_4$ with additive mixtures and to simultaneously identify the desorbed gases. The results are illustrated in Figure 2 and Table 1. Pure $NaBH_4$ has a

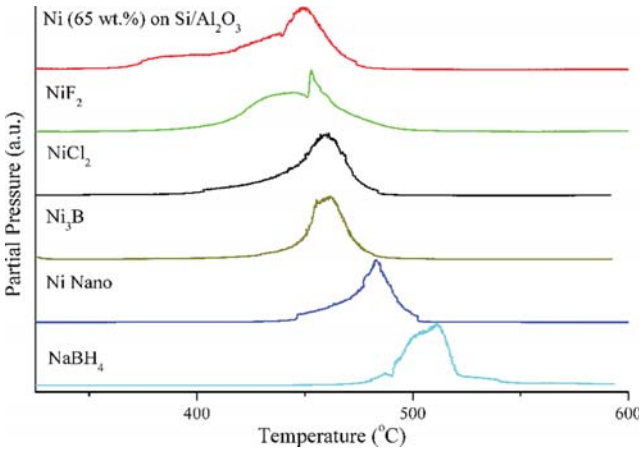

Figure 2. TPD analysis of $NaBH_4$ samples doped with Ni additives.

decomposition temperature of 510 °C (in vacuo), with the process occurring over a broad temperature range with the onset of H_2 desorption ca. 470 °C. Even the least effective additive, Ni nanoparticles, decreased the decomposition temperature by 27 °C. The only gas detected during the RGA experiment was H_2. Analysis of $NaBH_4$ milled with Ni containing additives demonstrates a decrease in decomposition temperature for all samples, with the most effective being Ni (65 wt %) on Si/Al_2O_3 (449 °C), a decrease of over 60 °C. RGA analysis of the desorption products indicated that H_2 is the only gas evolved during the process. The absence of borane derivatives promotes the idea that reversibility is possible as the products are not B-deficient. Additionally, these systems may become fuel sources for PEM fuel cells, which are easily poisoned by boranes and become inoperable.

Table 1 also includes the decomposition temperatures measured by TPD of $NaBH_4$ milled with the other additives studied. These results are presented in Figures S4–S6 in the Supporting Information. Although this publication is focused on Ni-containing additives, it must be mentioned that Pd actually has the largest effect on decomposition temperature, with maximum decomposition occurring at 420 °C. The catalytic activity of Pd toward the thermal decomposition of metal hydrides has been sparse, although Huang et al. calculated that Pd would have the greatest destabilizing effect on $NaAlH_4$ by the formation of a Pd_8Al_{21} alloy.[16] Recently, Weng et al. discovered that Pd nanoparticles enhance the reversible hydrogenation of $LiBH_4/MgH_2$ composites by the formation of Mg_6Pd,[17] whereas Xu et al. reduced the decomposition temperature of $LiBH_4$ with carbon-supported Pd (10 wt %) to ca. 280 °C.[18] The active Pd species formed during the decomposition of $NaBH_4$ and $LiBH_4$ is likely to be a Pd_xB_y alloy such as Pd_3B or Pd_5B_2 previously characterized by PXD, along with the amorphous boride Pd_2B.[19] The formation of a TM_xB_y alloy during decomposition of borohydrides with TMs is analogous to the $NaAlH_4$ with $TiCl_3$ system, where Ti_3Al has been identified as the active species during decomposition.[20,21] In this study, cycling experiments performed on $NaBH_4$ with Ni particles upheld this theory with the identification of Ni_3B by PXD. This phenomenon also explains why the Ni-containing additives, Ni_3B and $NiCl_2$, are the most efficient additives after Pd. In general, the most efficient category of additive for reducing the decomposition temperature of $NaBH_4$ is the boride- and chloride-containing compounds. Nanoparticles seem to be the least effective, with the majority causing a stabilization of $NaBH_4$, especially Fe and Cr nanoparticles, which increase the temperature of decomposition.

3.3. Cycling Studies. As described in Table 1, Ni-containing additives have been found to be very effective at decreasing the temperature of decomposition for $NaBH_4$. As such, the five mixtures of Ni-containing $NaBH_4$ were cycled four times in a Sieverts-type PCT apparatus. Each cycle was composed of a decomposition step under initial vacuum, followed by hydrogenation at 100 bar H_2 pressure. The decomposition process was carried out at temperatures of at least 5 °C higher than those measured by TPD (Table 1). The temperatures employed for rehydrogenation were below those measured for decomposition of the starting material, as measured by TPD. The time between each step was ~24 h. This did not allow each process to reach a constant pressure plateau, although the ultimate goal of these studies was to determine if reversible hydrogenation was possible and whether cycling of $NaBH_4$ with additives improved reversibility over consecutive cycles. After four cycles, the products removed from the sample holder were generally two distinct phases, one being a white powder and the other being dark. Both phases were analyzed separately by PXD unless the two phases were accidentally mixed while being removed from the sample vials (see Supporting Information (SI) for all PXDs, Figures S7–S11). The composition of each phase was studied by PXD to define the activity of the Ni additive during the process and determine whether the byproducts allow for efficient cycling. In all cases, it was found that the majority of the composition of the white powder was NaH with small quantities of Na, whereas the dark material consisted of Ni-containing species along with NaH and Na. There was no indication that reformation of $NaBH_4$ had occurred. The identification of NaH and Na in the products was expected due to the fact that Na is the decomposition product of $NaBH_4$, and the synthesis of NaH by hydrogenation of metallic Na has been reported since 1958 at 150 bar.[22] This reaction was also noted to occur at 300 °C with 2 to 3 bar H_2 by Dymova and Vysheslavtsev.[23] NaH

dx.doi.org/10.1021/jp312105w | J. Phys. Chem. C XXXX, XXX, XXX–XXX

Table 2. PCT Hydrogenation and Dehydrogenation Cycling Studies of $NaBH_4$ Milled with Additives (wt % H_2)[a]

	Ni		$NiCl_2$		Ni (65 wt %) on Si and Al_2O_3		Ni_3B		NiF_2	
cycle	desorb 490 °C	absorb 427 °C	desorb 514 °C	absorb 430 °C	desorb 494 °C	absorb 430 °C	desorb 460 °C	absorb 414 °C	desorb 460 °C	absorb 300 °C
1	0.25	0.09	0.25	0.06	0.23	0.07	1.45	0.41	0.16	0
2	0.17	0.35	1.48	0.47	0.17	0.39	0.28	0.03	0.03	0.02
3	0.05	0.97	0.05	0.33	0.07	0.06	0.04	0.33	0.02	0.04
4	0.02	0.20	0.03	0.08	0.03	0.30	0.05	0.21	0.02	0

[a]Desorption undertaken under initial vacuum. Absorption undertaken at ~100 bar H2.

typically decomposes to the elements above 400 °C (ΔH_{dec} = −114 kJ/mol H_2) without additives.[24] This has been reduced drastically above 130 °C, utilizing mixtures of NaH, Al, and Si with an associated reaction enthalpy of 2 kJ/mol H_2.[25] Hence it was anticipated that a similar process may take place within the $NaBH_4$ system with the reformation of $NaBH_4$.

The products after the fourth hydrogenation of $NaBH_4$ with Ni (65 wt %) on Si/Al_2O_3 were ground together and analyzed by DSC/TGA measurements. The results depicted an endothermic peak at 364 °C with a concomitant mass loss of 2 wt %. Assuming that all Na atoms in the decomposition products were hydrogenated to NaH, a maximum of 2.3 wt % H_2 would be available for desorption. This implies that 87% conversion of Na to NaH was achieved. The Ni species contained in this matrix after thermal treatment is not as efficient at reducing the decomposition temperature of NaH as the group IV additives reported by Nwakwuo et al.[25] The residual material from the DSC/TGA experiment was inspected thereafter, and the presence of elemental Na in the sample holder was determined. Quantification of Na was inhibited by the small sample size required for DSC and the tackiness of the metal. A separate identical PCT experiment was carried out where the products of the first decomposition were collected to ensure that the main product was Na. A lustrous, sticky, metallic substance was removed from the sample holder, rendering the loading of a glass capillary for PXD analysis impossible. This substance reacted violently with water. This ensures that the NaH observed after cycling is due to the hydrogenation of Na.

The hydrogenation products after four cycles of $NaBH_4$ with Ni (65 wt %) on Si/Al_2O_3 additive were identified by PXD. The analysis of the diffraction pattern for the white phase allowed the identification of NaH with some Na, whereas a few peaks were unidentifiable. The PXD of the predominantly dark material recovered contained some NaH and Na but also a large distribution of other Ni-containing compounds including Ni_6Si_2B, $Al_{1.1}Ni_{0.9}$, Ni_3B, Ni_2B, and metallic Ni. Other unidentifiable phases were also present between 2θ = 7 and 40°. The formation of these highly stable metal boride products is to be expected after heat treatment; for example, Ni_6Si_2B is synthesized by the heating of Ni, Si, and B powders at 900 °C. Although the temperatures are not that extreme, the formation is still likely to occur.[26]

The white material collected after the cycling of $NiCl_2$ doped $NaBH_4$ was analyzed by PXD. Apart from NaH and some Na, a small quantity of NaCl, residual $NaBH_4$, and miniscule quantities of NaOH were observed. The latter most likely appears to be due to reaction of the sample with the glue used to seal the capillary during PXD sample preparation. When this powder was mixed with the dark material, the same composition was present, excluding NaOH. In addition, Ni_2B and $NiH_{0.6}$ were detected in this mixture. The mixed product was analyzed by TPD, and the only significant gas detected was H_2, released gradually from 150 °C with a maximum desorption at 379 °C. Inspection of the sample holder after desorption revealed a ring of Na around the gasket and a black powder at the bottom of the vessel, which PXD measurements identified as containing mainly Ni_4B_3 and NaCl. The $NaBH_4$ with NiF_2-cycled material exhibited very similar features to the $NiCl_2$ system when analyzed by PXD. The white portion contained NaH, Na, and residual $NaBH_4$, whereas the dark matter contained $NaBH_4$, NaF, Ni_3B_4, and other NiB analogues. The sodium halide formation within these two systems likely occurs during the first decomposition of the material. It has been proposed that the formation of sodium halides plays an important role in promoting the dehydrogenation of $NaBH_4$ and may act as a nucleation center for the formation of NaH and Na.[14] The decrease in decomposition temperature obtained by the addition of the Ni halides on $NaBH_4$ is therefore aided by the formation of the Na halide, although it is also noticeable that these halides did not promote the hydrogenation process.

The PXD pattern of the mixed material from $NaBH_4$ with Ni_3B additive contained very similar components to those observed for the material with $NiCl_2$ additive (minus NaCl). The striking result of the analysis was that Ni had changed oxidation states from Ni_3B to Ni_2B. This can be attributed to the formation of elemental B during the decomposition of $NaBH_4$, which is free to react with Ni_3B during thermal treatment.

The cycling of $NaBH_4$ with Ni nanoparticles was halted after the fourth cycle to determine the products of decomposition. The sample holder contained two phases that were ground together. The PXD pattern identified the majority phase as NaH with Na and a miniscule amount of $NaBH_4$. Hydrogenation was then carried out, and the product was principally NaH with a much decreased amount of Na and a negligible quantity of $NaBH_4$. The Ni nanoparticles that were observed in the PXD pattern of the original milled material were not identifiable after cycling. Instead, Ni_3B was observed, indicating once more that the Ni reacts with the B formed during decomposition. This Ni_3B then becomes the active Ni species in the mixture to aid the decomposition process.

Evidently, although the Ni additives reduce the kinetic barrier required for $NaBH_4$ to decompose, they are not able to aid the reverse process. The inefficiency may lie in the initial decomposition process. The materials are initially milled together, allowing the Ni additives to mix with the fine particles of $NaBH_4$, aiding the decomposition process. Upon decomposition, elemental Na is formed that has a melting point of 98 °C and ΔH_{vap}= 97 kJ mol^{-1}, which is very low compared with other metals.[27] During decomposition, the high temper-

dx.doi.org/10.1021/jp312105w | J. Phys. Chem. C XXXX, XXX, XXX−XXX

atures evaporate the Na, which is then deposited on the walls of the sample tube and gasket upon cooling. Na also has a relatively high surface tension of 200.2 dyn cm^{-1} at 98 °C[28] (H_2O (100 °C) = 58.85 dyn cm^{-1} and Hg (15 °C) = 487 dyn cm^{-1}),[27] so when in the molten state the particles agglomerate, forming beads. Both of these physical properties suggest that upon cooling the B and the Ni additives are not in direct contact with the Na, thus hindering the reversibility of the material. The evaporation of Na causes the NaH to be formed further up the sample holder during hydrogenation, which explains the observation of the two distinct phases after cycling.

The PCT data measured over four cycles are illustrated in Table 2. It is recognizable that total decomposition has not occurred after the first desorption, even though the experiments were conducted at higher temperatures than those recorded for the decomposition by TPD measurements (Table 1). The extremely slow kinetics of the thermal decomposition of $NaBH_4$ means that the full dehydrogenation of the material is unlikely over a period of a few days, although the majority would be expected to be divulged over a longer period of time. Ni_3B greatly enhanced the desorption kinetics with a corresponding mass loss of 1.45 wt % H_2 in the first cycle compared with an average of 0.25 wt % for the other Ni additives. The H_2 released in additional desorptions does not increase over consecutive cycles, denoting that the activity of the additive does not increase over time. It is beneficial to notice that some H_2 absorption occurred during the reverse cycle, with each system having recorded a distinct decrease in H_2 pressure over time, the largest of which was 0.97 wt % H_2, measured on the third cycle of Ni-enhanced $NaBH_4$. It is clear from the PXD measurements mentioned in the previous section that $NaBH_4$ is not the product of these hydrogenation steps but rather NaH (Figures S7−S11 in the Supporting Information).

4. CONCLUSIONS

$NaBH_4$ has been milled with a variety of additives to investigate the effects on the temperatures required for thermal desorption of H_2. It has been established that Ni-containing additives significantly enhance the thermal desorption of H_2 by at least 60 °C (Ni (65 wt %) on Si/Al_2O_3). The prosperity of these results inspired a PCT cycling study of these materials to determine if reversibility ensues. It has been previously observed that cycling of metal hydrides with additives often promotes the formation of a reactive intermediate that enhances the reversibility of the material.[14] After four cycles, no improvement in reversibility of $NaBH_4$ with Ni-containing additives was observed. Nevertheless, our knowledge of the effect of additives during these processes has significantly improved. Ni reacts with B evolved during thermal decomposition to form Ni_xB_y species including Ni_3B, Ni_2B, and Ni_3B_4. These species are believed to improve the thermodynamics of the entailed processes. Some absorption of H_2 was determined to occur up to 0.97 wt % after cycle three, although PXD studies conclude that the major product was NaH.

We also included a catalyst screening study of $NaBH_4$ with a variety of nanoparticles, chlorides, borides, and mesoporous materials. The most effective was found to be Pd nanoparticles, which have a desorption temperature of 420 °C, a decrease of at least 85 °C. This process is most likely enabled by the formation of a Pd_xB_y reactive intermediate.

Overall, this study has developed our understanding of the thermal decomposition of $NaBH_4$ mixed with additives, which to date has not been reported in the literature. Even with the most effective additives, the temperatures required for desorption of H_2 are too high for commercial applications and cycling is extremely inefficient due to the slow kinetics. The formation of NaH as a hydrogenation product is also unfavorable due to its thermal stability and the requirement for it to react with the B containing compounds formed upon decomposition. No gaseous boranes were detected during decomposition, ensuring that no poisonous materials would be released if these mixtures were to be used for H_2 storage applications.

■ ASSOCIATED CONTENT

Supporting Information

PXD patterns of $NaBH_4$ milled with nanoparticles, mesoporous catalysts, transition-metal chlorides and transition-metal borides; TPD analysis of $NaBH_4$ samples doped with nanoparticles, transition-metal chlorides, mesoporous powders and transition-metal borides; and PXD patterns of $NaBH_4$ milled with Ni nanoparticles, NiF_2, Ni_3B, $NiCl_2$, and Ni (65 wt %) on Si/Al_2O_3 after cycling studies. This material is available free of charge via the Internet at http://pubs.acs.org.

■ AUTHOR INFORMATION

Corresponding Author

*Tel: +47 63806181. Fax: +47 63810920. E-mail: terry.humphries@ife.no.

Notes

The authors declare no competing financial interest.

■ ACKNOWLEDGMENTS

We acknowledge Dr. Christoph Frommen for his scientific input and the Research Council of Norway for financial assistance. The E.U. collaborative project SSH2S (256653) is gratefully acknowledged for partial funding of this work.

■ ABBREVIATIONS

DSC, differential scanning calorimetry; FT-IR, Fourier transform infrared spectroscopy; PCT, pressure composition temperature; PXD, powder X-ray diffraction; RGA, residual gas analyzer; TGA, thermogravimetric analysis; TPD, temperature-programmed desorption

■ REFERENCES

(1) Satyapal, S.; Petrovic, J.; Thomas, G. *Sci. Am.* **2007**, *296*, 80.
(2) http://www1.eere.energy.gov/hydrogenandfuelcells/mypp/pdfs/storage.pdf (accessed June 12, 2012).
(3) Bogdanovic, B.; Schwickardi, M. *J. Alloys Compd.* **1997**, *253*, 1.
(4) Roennebro, E. *Curr. Opin. Solid State Mater. Sci.* **2011**, *15*, 44.
(5) Manna, J.; Vashistha, M.; Sharma, P. *Int. J. Energy Clean Environ.* **2010**, *11*, 65.
(6) Santos, D. M. F.; Sequeira, C. A. C. *Renewable Sustainable Energy Rev.* **2011**, *15*, 3980.
(7) Li, H. W.; Yan, Y. G.; Orimo, S.; Zuttel, A.; Jensen, C. M. *Energies* **2011**, *4*, 185.
(8) Rude, L. H.; Nielsen, T. K.; Ravnsbaek, D. B.; Boesenberg, U.; Ley, M. B.; Richter, B.; Arnbjerg, L. M.; Dornheim, M.; Filinchuk, Y.; Besenbacher, F.; Jensen, T. R. *Phys. Status Solidi A* **2011**, *208*, 1754.
(9) Martelli, P.; Caputo, R.; Remhof, A.; Mauron, P.; Borgschulte, A.; Züttel, A. *J. Phys. Chem. C* **2010**, *114*, 7173.
(10) Bogdanovic, B.; Schwickardi, M. *Appl. Phys. A: Mater. Sci. Process.* **2001**, *72*, 221.

(11) Liu, X. F.; McGrady, G. S.; Langmi, H. W.; Jensen, C. M. *J. Am. Chem. Soc.* **2009**, *131*, 5032.
(12) Graetz, J.; Wegrzyn, J.; Reilly, J. J. *J. Am. Chem. Soc.* **2008**, *130*, 17790.
(13) Saldan, I. *Cent. Eur. J. Chem.* **2011**, *9*, 761.
(14) Mao, J.; Guo, Z.; Nevirkovets, I. P.; Liu, H. K.; Dou, S. X. *J. Phys. Chem. C* **2012**, *116*, 1596.
(15) Kapfenberger, C.; Hofmann, K.; Albert, B. *Solid State Sci.* **2003**, *5*, 925.
(16) Huang, C. K.; Zhao, Y. J.; Sun, T.; Guo, J.; Sun, L. X.; Zhu, M. *J. Phys. Chem. C* **2009**, *113*, 9936.
(17) Weng, B. C.; Yu, X. B.; Wu, Z.; Li, Z. L.; Huang, T. S.; Xu, N. X.; Ni, J. *J. Alloys Compd.* **2010**, *503*, 345.
(18) Xu, J.; Yu, X. B.; Ni, J.; Zou, Z. Q.; Li, Z. L.; Yang, H. *Dalton Trans.* **2009**, 8386.
(19) Beck, M.; Ellner, M.; Mittemeijer, E. J. *Powder Diffr.* **2001**, *16*, 98.
(20) Brinks, H. W.; Jensen, C. M.; Srinivasan, S. S.; Hauback, B. C.; Blanchard, D.; Murphy, K. *J. Alloys Compd.* **2004**, *376*, 215.
(21) Brinks, H. W.; Hauback, B. C.; Srinivasan, S. S.; Jensen, C. M. *J. Phys. Chem. B* **2005**, *109*, 15780.
(22) Nenitzescu, C. D.; Badea, F. *Bul. Inst. Politeh. Bucuresti* **1958**, *20*, 93.
(23) Dymova, T. N.; Vysheslavtsev, A. A. *Zh. Neorg. Khim.* **1960**, *5*, 2153.
(24) Banus, D. M.; McSharry, J. J.; Sullivan, E. A. *J. Am. Chem. Soc.* **1955**, *77*, 2007.
(25) Nwakwuo, C. C.; Eigen, N.; Dornheim, M.; Bormann, R. *Renewable Energy* **2012**, *43*, 172.
(26) Rundqvist, S.; Jellinek, F. *Acta Chem. Scand.* **1959**, *13*, 425.
(27) Lange, N. A. *Lange's Handbook of Chemistry*, 11th ed.; McGraw-Hill: New York, 1973.
(28) Jordan, D.; Lane, J. *Aust. J. Chem.* **1965**, *18*, 1711.